Proceedings World Geothermal Congress 2015
Melbourne, Australia, 19-25 April 2015

Resistivity Imaging of the Santa Maria Sector and the Northern Zone of Las Pailas Geothermal Area, Costa Rica, Using Joint 1D Inversion of Tdem and Mt Data

Diego Badilla Elizondo

ICE, P.O. Box 10032, Sabana Norte, San José, Costa Rica

dbadillae@ice.go.cr

Keywords: resistivity, inversion, static shift, permeability, alteration, reservoir.

ABSTRACT

In this work, geophysical exploration data from MT and TDEM surveys are processed, interpreted and discussed to explain the electrical resistivity of the subsurface in two specific areas located to the north and east of Las Pailas Geothermal Field in Costa Rica. The static shift problem of MT data is solved by inverting jointly both TDEM and MT data. Seven profiles are analysed, based on 1D models from 22 MT and 19 TDEM soundings. Resistivity cross sections and iso-resistivity maps were compiled from the 1D models of the inverted TDEM and MT data. The main idea was to analyse the subsurface resistivity structure of those areas and also to compare the results with a discontinuity known as NF7, trying to see if the existing MT and TDEM data could reveal a more detailed model about the zone that can be of use in future expansion of the production field. The main result of the survey is the probably confirmation of the NF7 structure in the northern side of the survey area and in Santa María sector. It was also an important fact to see a low resistivity body (deep conductor) to the northern part of the study area and in Santa María sector which is interpreted as a heat source.

1. INTRODUCTION

Geophysical exploration for geothermal resources has become an essential tool that together with geochemistry and geology plays a very important role in the exploration campaign of a geothermal area.

Resistivity is directly related to the properties of interest, like salinity, temperature, porosity (permeability) and alteration. To a great extent, these parameters characterize the reservoir (Hersir and Árnason, 2009). This capacity of the resistivity has made from the electromagnetic methods the most powerful geophysical method in geothermal exploration.

Las Pailas Geothermal Area is located on the southern part of the Rincón de la Vieja Volcano. The Rincón de la Vieja volcano belongs to the Guanacaste volcanic range, and is located between the Miravalles and Orosí volcanoes. Las Pailas Geothermal Field is now producing 35 MW electrical power, but the idea is to increase the production of the field in a few years.

The objective of this work was to get to know in more details the subsurface resistivity structure to the north and east of Las Pailas Geothermal Field, specifically in the zone of Santa Maria which is located 3 km to the east of the well #2 and to the north of well #2, as shown in Figure 5.

The work was done using data of two electromagnetic methods: the magnetotelluric (MT) and the time domain electromagnetic (TDEM). Data were collected by the personal of the Geophysics' Department of the Costa Rican Electricity Company (ICE) in collaboration with the Geothermal Resources Service Center (CSRG). These data were processed, edited and finally modelled to produce different results like maps and cross sections to represent the subsurface resistivity structure of the area.

This survey becomes very important for the CSRG because the area in study is a part of the Las Pailas Geothermal Field, and the results could help to decide if the zone would be profitable for a future extension of the geothermal field.

The survey was done on profiles mainly across one important discontinuity of the zone, known as NF7, according to the existing MT and TDEM data. This structure was suggested in the geothermal model proposed by the Geothermal Resources Service Center (CSRG) Geology Department, and by the consulting company West Japan Engineering Consultants (WestJEC).

In this specific project, we are using 1D inversion models of the rotationally invariant determinant of the apparent resistivity of MT. The main reason for that is because the time that we had to process and analyse the data was not enough to do 2D or 3D inversion.

Preliminary model calculations and reported geothermal industry experience indicate that smooth, minimum structure 1D inversion of the rotationally invariant determinant data of MT can reproduce complex 3D resistivity structures, while 1D inversion of either xy or yx modes can give misleading results (Árnason, et al, 2010).

2. RESISTIVITY OF ROCKS

The specific resistivity, ρ, is an electric characteristic that depends on the material and it is measured in Ohm-meter (Ωm).

2.1 Factors affecting electrical resistivity of water-bearing rocks

In geothermal areas the rocks are water-saturated. The ionic conduction in this condition depends on the number and mobility of ions and on the rock matrix, because conduction is also defined by the connectivity of the flow paths through the rock. The main factors that control the resistivity of rocks are temperature, porosity and permeability, salinity and water-rock interaction and alteration.

3. TDEM METHOD

3.1 Central loop transient electromagnetic method

In the central-loop TDEM sounding method, a current is induced in the ground by a time-varying magnetic field of a controlled magnitude generated by a source loop. A loop of wire is placed on the ground and a constant magnetic field of known strength is built up by transmitting a constant current into the loop (see Figure 1). The decaying magnetic field built induces electrical currents in the ground (Árnason, 2006a).

With this process, the current distribution in the ground generates a secondary magnetic field that decays with time. The decay rate of the secondary magnetic field, recorded as a function of time after the current in the transmitter loop is turned off, can therefore be interpreted in terms of the subsurface resistivity structure (Árnason, 1989).

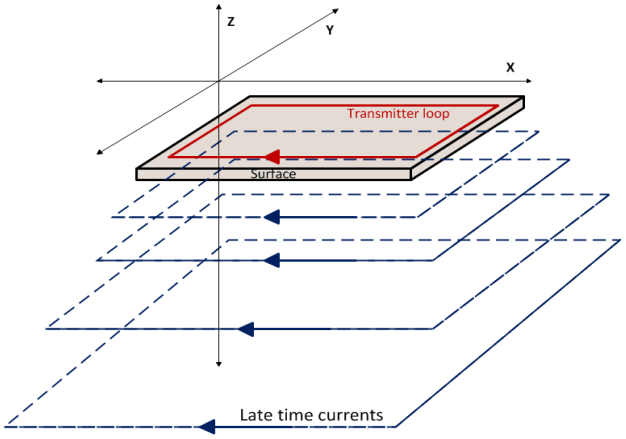

Figure 1: Current propagation, late time (modified from Rowland, 2002)

4. MT METHOD

4.1 Basic principles

The magnetotelluric (MT) technique involves measuring fluctuations in the earth natural electric, **E**, and magnetic, **B**, fields in orthogonal directions (see Figure 2) at the surface of the earth as a mean of determining the conductivity structure of the earth at depths ranging from a few tens of meters down to several hundreds of kilometres (Simpson and Bahr, 2005).

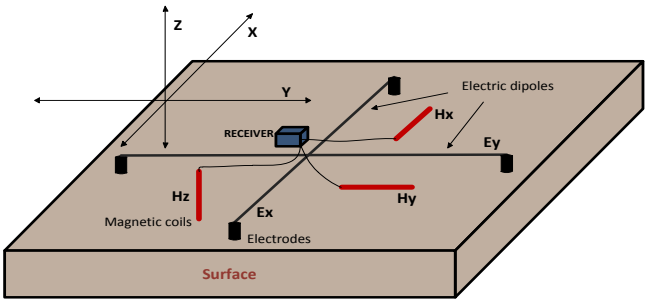

Figure 2: MT basic configuration (Phoenix Geophysics, 2009)

The principle of MT is based in the electromagnetic skin depth relation, which describes the exponential decay of electromagnetic fields as they diffuse into a medium. At a depth, δ(T), electromagnetic fields are attenuated to e^{-1} of their amplitudes at the surface of the Earth. This exponential decay of electromagnetic fields with increasing depth renders them insensitive to conductivity structures lying deeper than δ(T). Hence, in MT studies, electromagnetic skin depth is generally equated with the penetration depth of electromagnetic fields into the Earth.

$$\delta(T) = 500\sqrt{T\rho} \tag{1}$$

Where δ is the skin depth in m, ρ is the resistivity, or the average resistivity of an equivalent uniform half-space (Simpson and Bahr, 2005).

5. DATA PROCESSING AND INVERSION OF TDEM AND MT DATA

5.1 TDEM and MT data processing

To prepare the TDEM measured data for the inversion the first thing to do was to edit the soundings, for this a Unix based program called TEMX written by Árnason (2006a). It was specially created to manage files generated by the V8 from Phoenix Geophysics. It performed sacking of the measured values an outliers were thrown out. Finally the .inv file was created, later to be inverted.

For the MT data we used .edi files, which were the result of a processing of the data with software from Phoenix, like SSMT200 and MTeditor. The .edi files were transformed into Unix later to be used as an input to ISOR's software. For this purpose we used some routines like dos2unix, spec2edi and finally edi2ps to generate graphical files with the different curves. The processed data for all the MT soundings are given in Badilla (2011, Appendix 2).

5.2 Inversion of the data

In this work 1D inversion models of the rotationally invariant determinant of the apparent resistivity were used. The main reason for that is because the time that we have to process and analyse the data is not enough like to go through 2D or 3D inversion.

The most widely used inversion method, at least for inversion of geo-electric soundings, is the least-squares inversion method. In the case when the response depends non-linearly on the model parameters this method is referred to as non-linear least-squares inversion (Árnason, 1989).

In the joint inversion TDEM soundings are used to correct for the static shift problem of the MT stations. As already discussed TDEM soundings use only the magnetic field, which is relatively unaffected by those superficial and lateral distortions, to calculate the apparent resistivity of the site.

The software from ISOR known as TEMTD (Árnason, 2006b) was used to perform a joint 1D Occam inversion for the rotationally invariant determinant apparent resistivity and phase of the MT soundings and associated TDEM soundings and to get the final model of the data, and in this case it determines the best static shift parameter for the MT data. The 1D models of the joint inversion for all the TDEM and MT data are given in Badilla (2011, Appendix 3).

After getting the results of the joint inversion it was possible to create resistivity cross sections for all of the profiles using the routine TEMCROSS and the resistivity maps at different depths using the routine TEMRESD.

6. LAS PAILAS GEOTHERMAL AREA

6.1 Location and tectonic setting of the study area

The most important tectonic feature of the Central American region is the subduction of the Cocos plate under the Caribbean plate along the Middle American trench convergent margin, with rates of nearly 10 cm/year across the Costa Rican segment of the trench (DeMets et al., 1990). That interaction has generated an internal magmatic arc in which the Guanacaste Volcanic Range comprises its north-western segment.

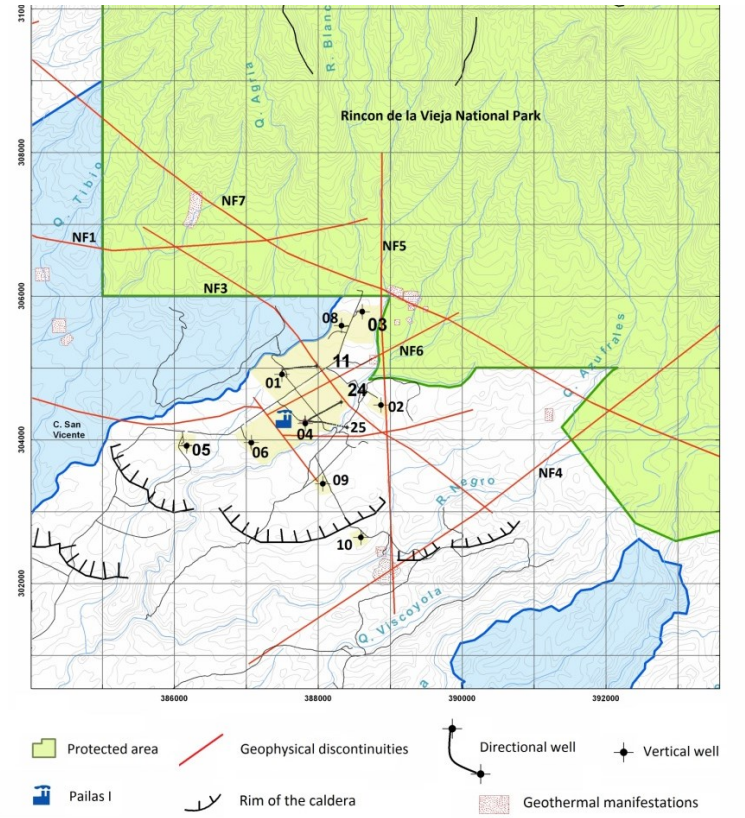

Figure 3: Structural setting of Las Pailas Geothermal Field(taken from ICE internal data and the department of geology of the CSRG)

6.2 Structural setting of the study area

Within Las Pailas geothermal area inferred faults and lineaments (Figure 3) were defined by a combination of factors including: morphology, field evidence (fractures), of hydrothermal alteration, gravimetric data and resistivity data (Chavarría, et al, 2010).

The structural setting is dominated by normal faults (GeothermEx, 2001), there are also several circular depressions identified that have been interpreted as possible borders of a caldera (GeothermEx, 2001). The main caldera structures suggested in the area Cañas Dulces and San Vicente. The Cañas Dulces caldera was formed on the south border by the Cañas Dulces and Torre hills, while the domes San Roque, Góngora and Fortuna are located in the central part of the structure. The San Vicente caldera is clearly defined on the south part, while other borders are not defined.

6.3 Geothermal manifestations

There are four important superficial geothermal manifestations on the Pacific volcano side called Las Hornillas, Borinquen, Las Pailas and San Jorge-Santa María (Figure 4), aligned in a NW-SE direction, parallel to the Rincón de la Vieja volcanic axis (Molina, 2000), a good confirmation of a structural control for the deep water circulation system in the zone.

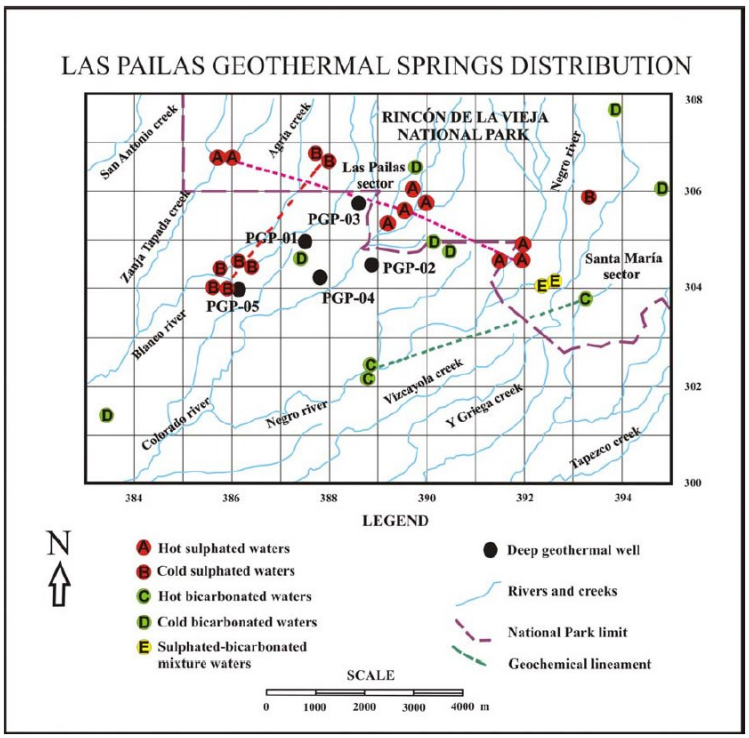

Figure 4: Geothermal manifestations in Las Pailas Geothermal area (taken from Barrantes, 2006)

The geothermal exploration in Las Pailas sector has revealed several manifestations. Most of them are inside Rincon de la Vieja national park. With some geochemical studies, thermal and cold springs have been characterized, as well as fumaroles with gas and steam emanations (Chavarría et al., 2006).

The hot sulphated waters (A) appear to be related to regional structures with different orientations. They include the Las Hornillas, Las Pailas and Santa María manifestations, which are aligned NW-SE and include fumaroles (88-93°C), hot springs (34-96°C) and mud pools (96°C). The cold sulphated waters (B) form a lineament perpendicular (NNE-SSW) to the volcanic axis, with temperatures between 15 and 25°C and are located in the vicinity of the Agria creek and an isolated point in Santa María sector. The hot bicarbonate waters (C) are located on a NE-SW lineament in the Negro river. They are meteoric waters with geothermal influence, and temperatures between 33 and 56°C. The cold bicarbonate waters (D) are distributed over many places. Their temperatures vary between 16 and 29°C. Finally, sulphated-bicarbonate mixture waters (E) are in the Santa María sector, with temperatures around 40°C, with variable chemical compositions with time; some sulphur deposits have formed (Barrantes, 2006).

7. RESULTS OF THE TDEM AND MT SURVEYS

Two small areas to the north-eastern zone of Las Pailas Geothermal Area are analysed here: the zone known as Santa Maria which is located 3km to the east of the well #2 (PGP#2) and the zone to the north of well #2 as we can appreciate in Figure 5. For this work, 22 MT and 19 TDEM soundings were used to create 7 different profiles across the structures known as NF7 and NF4 in Las Pailas Geothermal Area.

In the Figure 5 it is possible to see the location of the study area, showing the analysed profiles, the location of Las Pailas Geothermal Field, some of the production wells and the boundary of the Rincon de la Vieja National Park..

Initially, maps for the zstrike and tipper strike were created. Then, the resistivity cross sections were obtained using the resulting models for each sounding and in this report some cross sections down to 5000 m b.s.l. are shown. After that some iso-resistivity maps were created according to elevations of interest, but the maps shown in this document are only valid for the areas where the

profiles are located, but not for the area between them, because that is only an interpolation effect. All the resistivity cross sections and iso resistivity maps are given in a special report with appendices (Badilla, 2011).

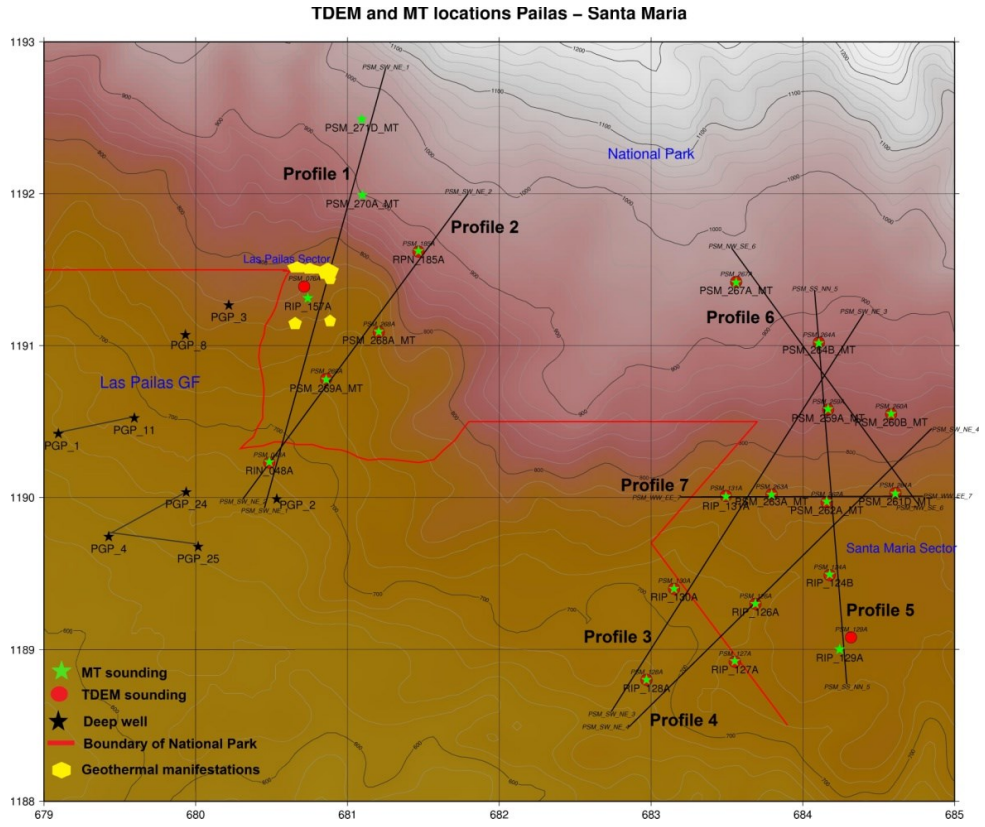

Figure 5: Location map of the study area

7.1 Interpretation of zstrike and tipper strike

The electrical strike direction is shown Figure 6 and Figure 7 for two different ranges of periods. The Zstrike always has 90° ambiguity, while the tipper strike which is based on the z component of the magnetic field does not include this ambiguity. The z component was only measured in relatively few soundings and that is the reason why the tipper doesn't appear for some MT soundings.

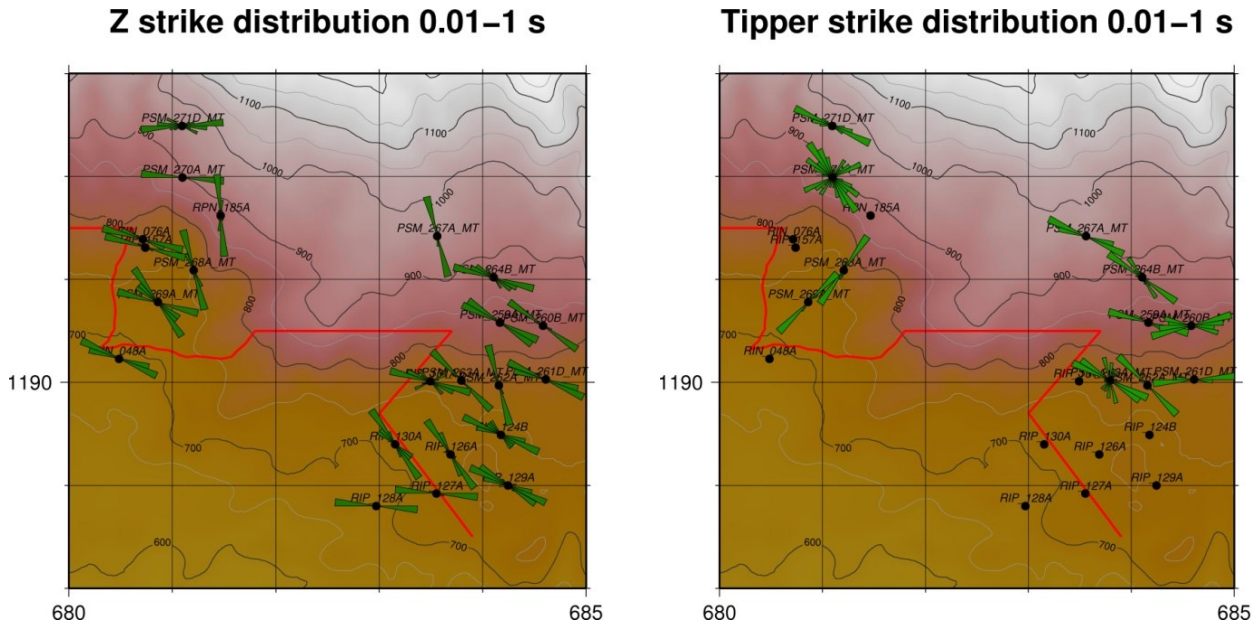

Figure 6: Rose diagram of the electrical strike based on Zstrike and Tipper strike for a period from 0.01 to 1 s. Black dots denote MT soundings. Red line marks the national park

In the Figure 6 a) and b) the Zstrike and tipper strike for frequencies between 1 and 100 Hz are shown, reflecting structures down to a depth of around 2 or 4 km. We can see how most of the soundings have a trend of -45° (azimuth) for both Zstrike and tipper, which agrees with the geological strike of the area. There are two soundings where the tipper strike is approximately 45° (-135°) and we could think that they are suggesting a structure in that direction, because they are very clearly oriented.

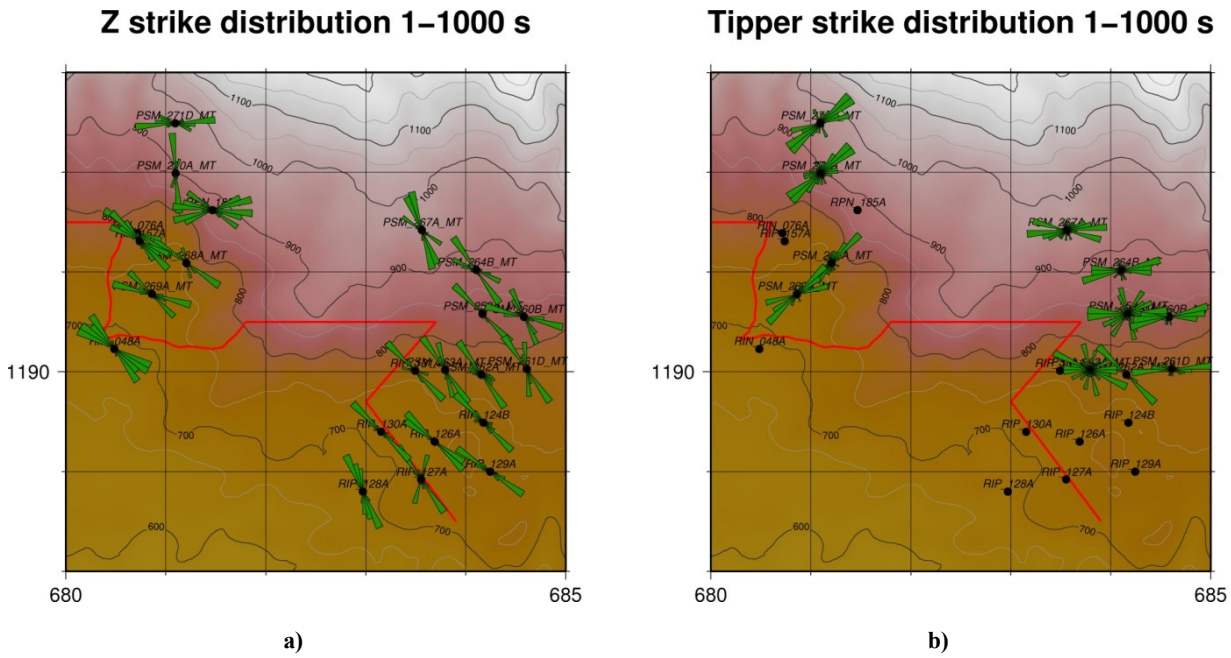

Figure 7: Rose diagram of the electrical strike based on Zstrike and Tipper strike for a period from 1 to 1000 s. Black dots denote MT soundings. Red line marks the national park

In the Figure 7 a) and b) we have the Zstrike and tipper strike for frequencies between 1 and 0.001 Hz, which represent greater depths. The Zstrike has the same value than for high frequencies because we constraint it according to the geological strike to avoid the ambiguity, but the tipper changes especially for the soundings in the profiles 1 and 2, and it seems that there is a structure suggesting those -45°, and it can be reliable because the 90° of ambiguity were eliminated with the use of the z component. In the zone of Santa María it seems that the tipper changes from -45° to -90° at shallow and deeper depths, respectively. It is important to see that the tipper strike for shallow depths (around 2 to 4km) is suggesting a structure intersection at around the sounding RPN_185A, which is located close to the heat source according to the resistivity model, and this could be acting as a pathway for fluid flow. In the same zone the tipper at greater depths suggests the presence of a deep structure running north-east south-west (-135°). This deep structure is probably a fracture in which fluids are flowing to the surface (up flow zone), which is being represented by the geothermal manifestations in the zone, as shown in Figure 5.

7.2 Resistivity cross sections

The resistivity cross-sections from 1D joint inversion of MT and TEM data show three major resistivity structures. A high-resistivity uppermost layer with values approximately higher than 50 Ωm. Then, a conductive cap with values lower than 10 Ωm and in the bottom a high resistivity cap with values higher than 100 Ωm. Between these two last layers there is always a intermediate resistivity cap seen in all of the cross sections.

In the resistivity cross section of the profile 1 shown in Figure 8 it is possible to see in the shallow part a high resistivity cap ($\rho > 50$ Ωm), associated to unaltered rocks. Then, a well-defined low resistivity cap (from 1 Ωm up to 10 Ωm) which is interpreted as the smectite-zeolite clay cap and related to temperatures between 100°C and 200°C (Árnason et al., 2000). It is possible to see low resistivity in the very shallow part and around the sounding RIP_157A (PSM_157A), which is well correlated with some geothermal manifestations in the area as we can see in Figure 3, Figure 4 and Figure 5. Then, at around 400 m b.s.l., it is possible to see resistivities between 10 Ωm and 50 Ωm which could be associated with a smectite-chlorite mixed layer and with temperatures up to 230°C. After 1000 m b.s.l. a high resistivity body appears (resistivities higher than 100 Ωm) below soundings PSM_269A and RIP_157A (PSM_157A) and this might be interpreted as the high resistivity core, where alteration minerals as chlorite and epidote would be present. In Figure 8, it is clearly seen that below the soundings PSM_270A and PSM_271D, a low resistivity body appears after 2000 and 4000 m b.s.l., respectively, which could be associated to a heat source.

The Figure 9 shows the resistivity cross section of the profile 2 down to 5000 m b.s.l. It is possible to see a resistivity structure similar to the profile 1. The main facts in this cross section are the high resistivity core appearing at 1000 m b.s.l. which is correlated with the chlorite and epidote clays as in profile 1; and the deep conductor below the sounding PSM_185A (RPN_185A) below 2000 m b.s.l., which is well correlated with the conductor seen in the profile 1, representing what could be interpreted as the heat source.

In the Figure 10 we have the resistivity cross sections for the profile 3 down to 5000 m b.s.l. In this section we can see a resistivity structure similar to the profile 1 and 2, having in the shallow part a high resistivity cap (unaltered rocks), then a very low resistivity

cap associated with the smectite-zeolite clay cap and after 1000 m b.s.l. a high resistivity cap interpreted as the chlorite-epidote clay cap and with temperatures higher than 230 °C. With a deeper model it is possible to see how below 6000 m b.s.l. approximately, and in between soundings PSM_130A (RIP_130A) and PSM_131A (RIP_131A) an indicator of a deep conductor appears, which could be related as the heat source for that zone

The resistivity cross section of the profile 4 is shown in Figure 11 down to 5000 m b.s.l. The resistivity structure for this section is very similar to the profile 3 because we have the high-low-high model again and the three caps are still well defined. With a deeper model it is possible to see a deep conductor appearing again below 6000 m b.s.l., which is well correlated with the profile 3 and with a heat source, but also this could be a suggestion of the continuity of the structure NF7 shown in Figure 20, in that zone.

For the profiles 5, 6 and 7 of the Figure 5 it is possible to identify a resistivity structure very similar to the described above for the profiles 3 and 4, and that means that they are well correlated at least up to 5000 m b.s.l., but it is not possible to see a deep conductor like in profiles 3 and 4.

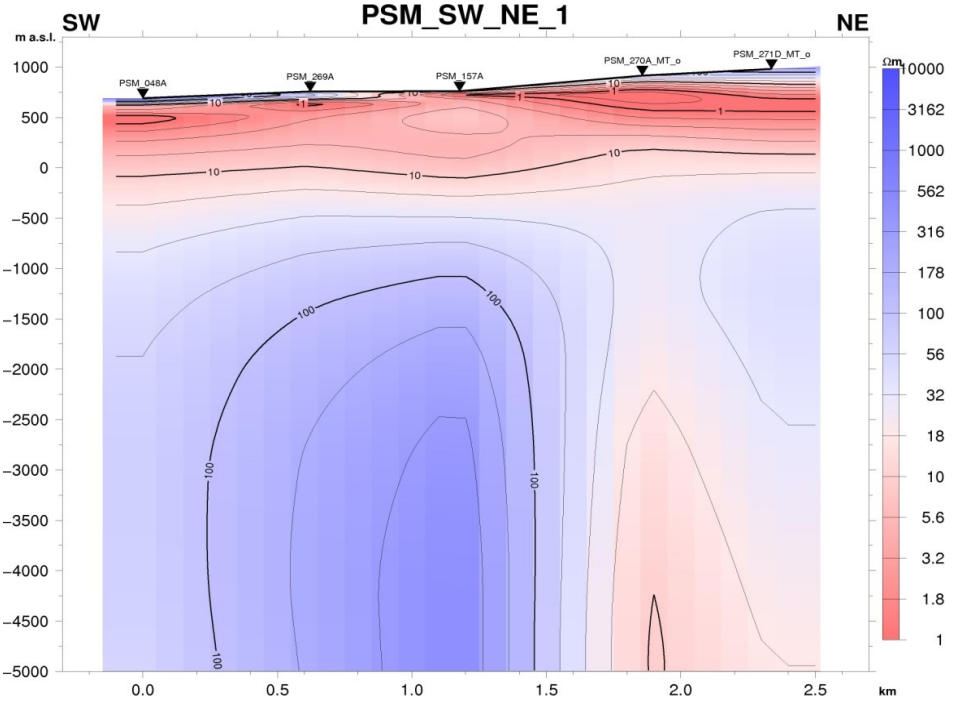

Figure 8: MT resistivity cross section PSM_SW_NE_01 down to 5000 m b.s.l.

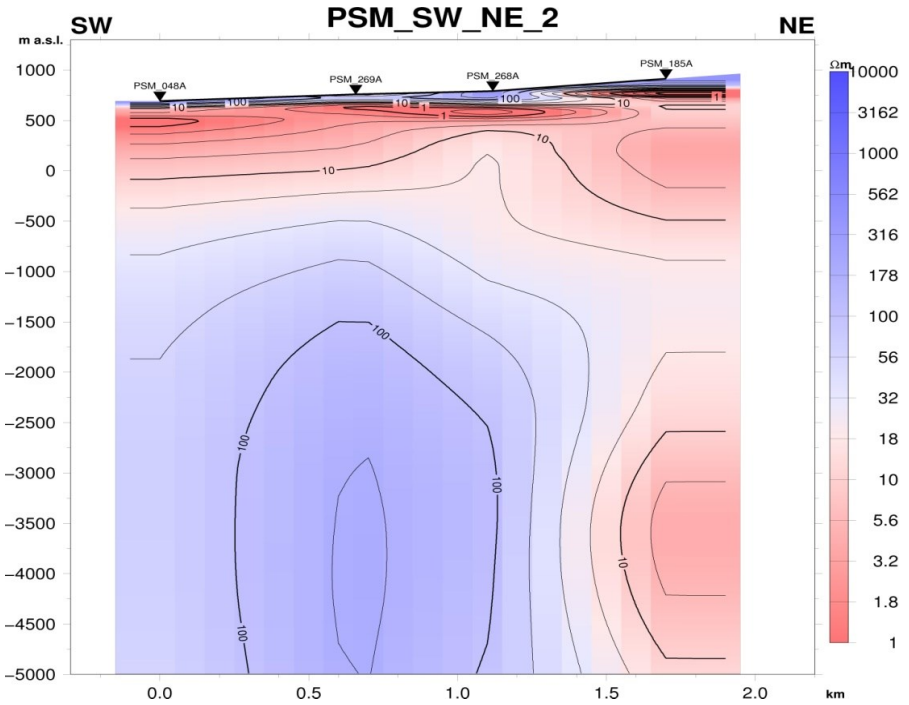

Figure 9: MT resistivity cross section PSM_SW_NE_02 down to 5000 m b.s.l.

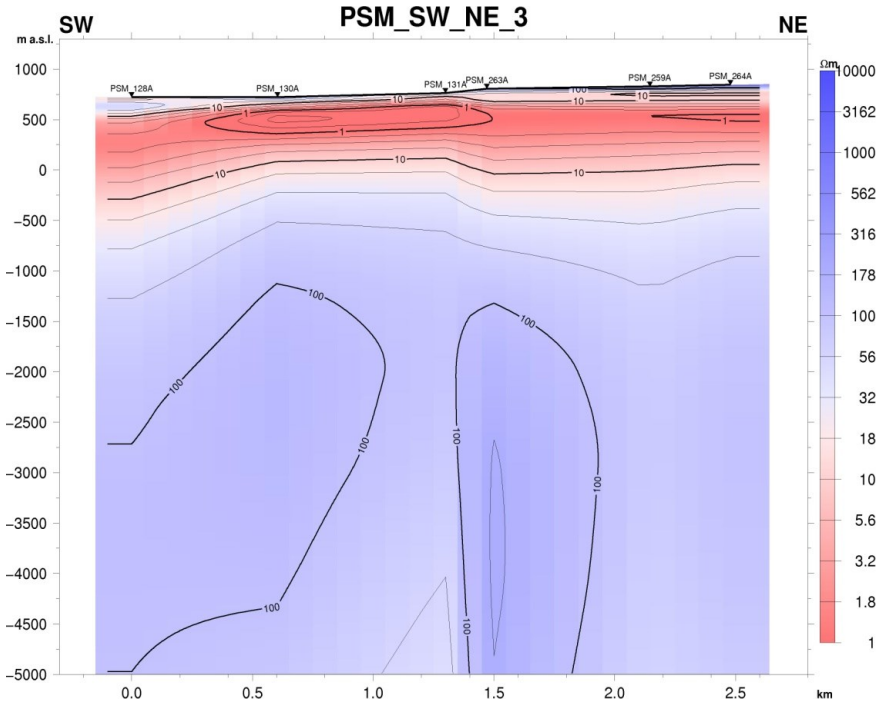

Figure 10: MT resistivity cross section PSM_SW_NE_03 down to 5000 m b.s.l.

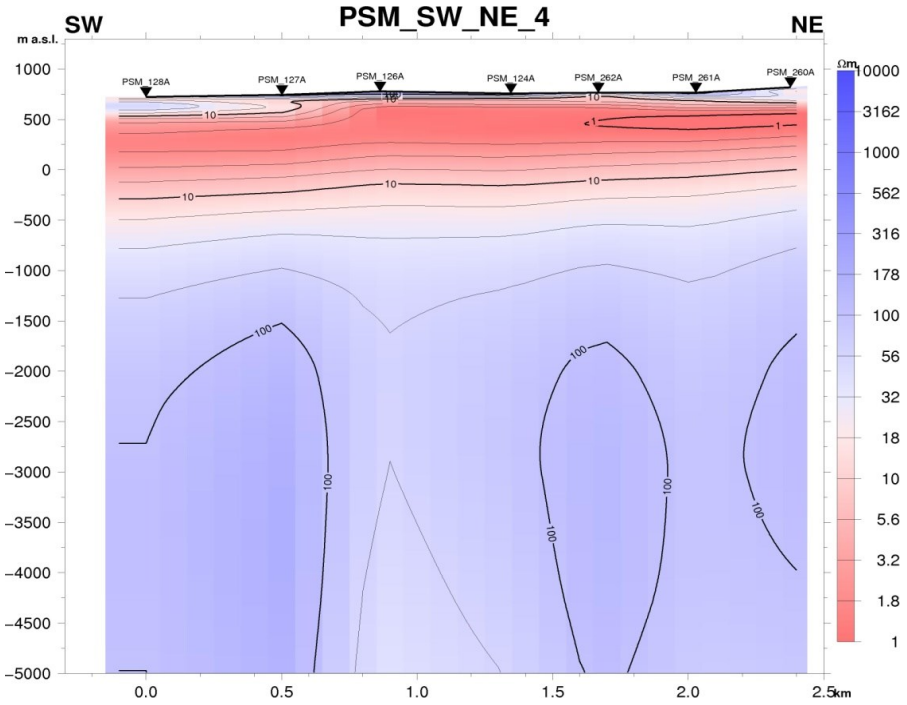

Figure 11: MT resistivity cross section PSM_SW_NE_04 down to 5000 m b.s.l.

7.2 Resistivity maps

Once all the cross sections were obtained, resistivity maps were created at different elevations.

In Figure 12 the resistivity map at 500 m a.s.l shows the distribution of probably smectite-zeolite clay cap, because a well-defined conductor is seen around that elevation with resistivity values characteristic for those alteration minerals and where it could be found temperatures between 100°C and 230°C.

Resistivities higher than 50 Ωm are seen in the major part of the map in Figure 13, what could interpreted as part of the high resistivity core, and that is associated with alteration minerals like chlorite and epidote and with temperatures higher than 230°C. Here we see lower resistivity in two soundings, indicating the deep conductor.

The resistivity map at 3000 m b.s.l is shown in Figure 14 and the most important fact that we can see there is the low resistivity body (deep conductor) to the northern part of the study area, which could be interpreted as a heat source and it is still appearing at 5000 m b.s.l. This is well correlated with the actual conceptual model of the area suggesting the location of the heat source in that zone. Note also an indication of low resistivity at depth in the Santa María Sector for these last two resistivity maps.

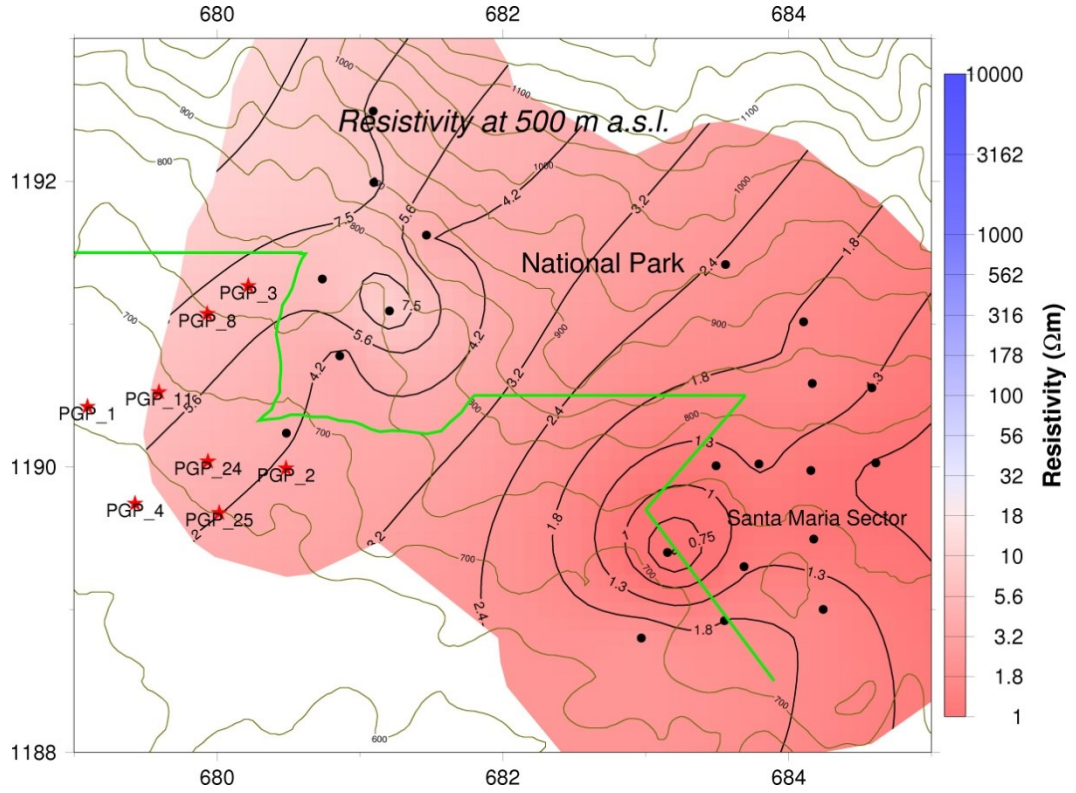

Figure 12: Resistivity map at 500 m a.s.l. Black dots denote MT soundings and red stars wells. Green line marks the national park

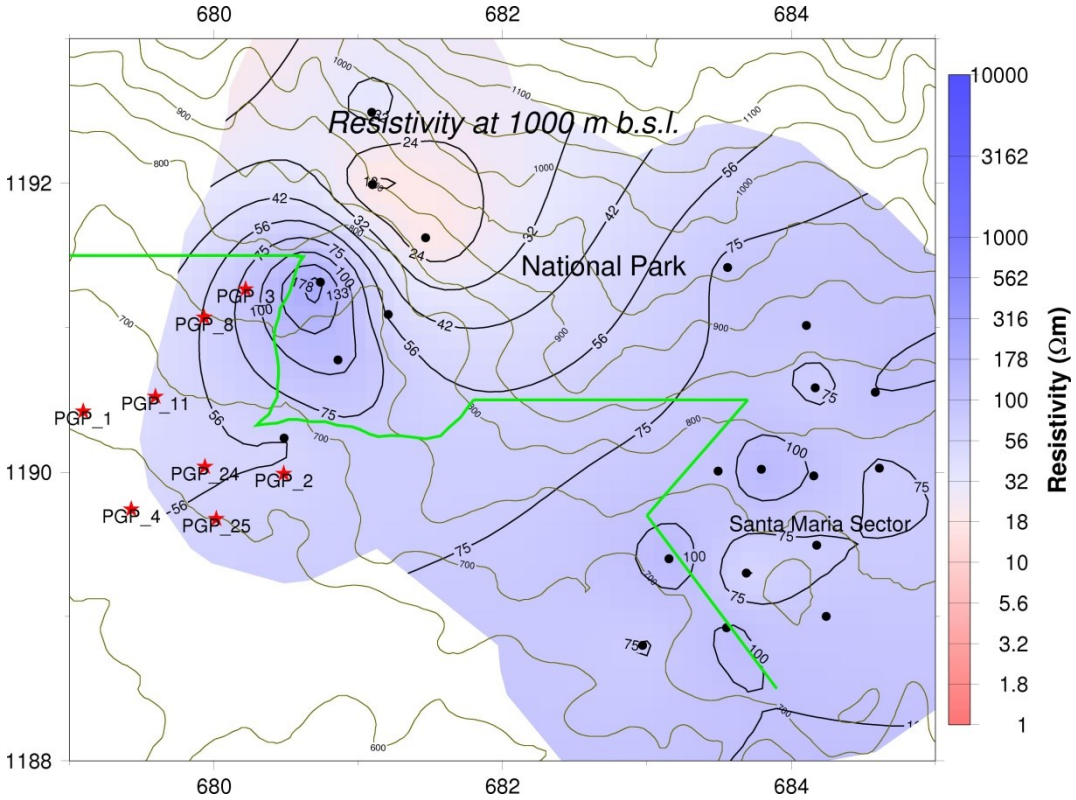

Figure 13: Resistivity map at 1000 m b.s.l. Black dots denote MT soundings and red stars wells. Green line marks the national park.

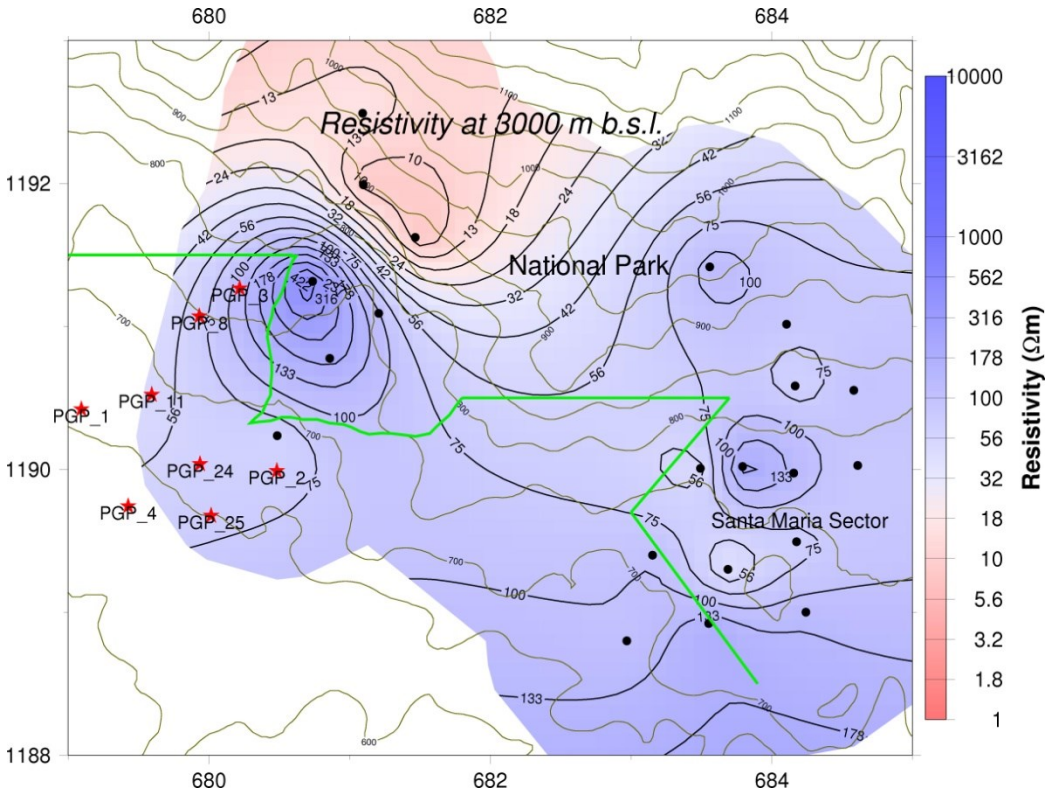

Figure 14: Resistivity map at 3000 m b.s.l. Black dots denote MT soundings and red stars wells. Green line marks the national park.

8. CONCLUSIONS AND RECOMENDATIONS

- A well-defined low resistivity conductor is detected at around 400 m depth in all of the resistivity cross-sections from 1D joint inversion of MT and TEM data, which is also shown in the resistivity map of 500 m.a.s.l., and this could be associated with smectite and zeolites clay cap. Resistivity increases after this first low resistivity cap and the resistivity at around 400 m.b.s.l shows values between 20 Ωm and 60 Ωm, approximately, which could be interpreted as part of the smectite-chlorite mixed layered. The low resistivity cap and the mixed layered clay zone are underlain by a high resistivity core. It represents a zone where chlorite and epidote are dominant alteration minerals. Provided there is equilibrium between alteration and present temperature the high resistivity zone indicates temperatures exceeding 230 °C.

- The resistivity maps show in the northern part in Las Pailas a deep laying conductor which could be associated with a deep sealed heat source. But also a similar conductor is detected at depth in the Santa María sector for profiles 3 and 4, which could be related with a heat source and with the continuity of the structure NF7 in that zone.

- The high resistivity zone shown in the maps at 1000 and 3000 m b.s.l and at around the soundings RIP_157 (PSM_157A) and PSM_269A is an important zone to analyse more in detail because the main geothermal manifestations are located there, which gives support to the hypothesis described above.

- Joint 1D inversion of MT and TDEM data solves the static shift problem of MT soundings giving a reliable model of the data.

- The tipper strike distribution for a period range from 0.01s to 1 s shown in Figure 6 b) and specifically for the soundings PSM_270A and PSM_271D agrees not only with the geological strike (running north-west south-east) but also with important changes in resistivity (south-west north-east) at around the sounding RPN_185A (PSM_185A) which are also associated to the suggested structure NF7 running north-west south-east.

- The tipper strike distribution (running south-west north-east) shown in Figure 7 b) for a period range from 1 to 1000 s, especially for soundings PSM_268A, PSM_269A, PSM_270A and PSM_271D can be interpreted with the resistivity maps at 1000 and 3000 m b.s.l. as a possible intersection of fractures acting as a pathway for fluid flow.

- Through the rose diagrams shown in Figure 6 and Figure 7 it was proved that there is a 90° of ambiguity in the Zstrike, because it was necessary to constrain the direction for the Zstrike to be in the direction of the geological strike; while it was not necessary in the tipper strike because this ambiguity is supressed by the use of the z component of the magnetic field, and we can see in the Figure 6 b) how it agrees with the geological strike (running north-west south-east).

REFERENCES

Árnason, K., 1989: *Central-loop transient electromagnetic sounding over a horizontally layered earth*. Orkustofnun, Reykjavík, report OS-89032/JHD-06, 129 pp.

Árnason, K., 2006a: *TemX. A graphically interactive program for processing central-loop TEM data, a short manual.* ÍSOR – Iceland GeoSurvey, Reykjavík, 10 pp.

Árnason, K., 2006b: *TEMTD. A program for 1D inversion of central-loop TEM and MT data, a short manual.* ÍSOR – Iceland GeoSurvey, Reykjavík, 16 pp.

Árnason, K., Eysteinsson, H., and Hersir, G.P. 2010: Joint 1D inversion of TEM and MT data and 3D inversion ofMT data in the Hengill area, SW Iceland. *Geothermics, 39,* 13–34.

Árnason, K., Karlsdóttir, R., Eysteinsson, H., Flóvenz, Ó.G., and Gudlaugsson, S.Th., 2000: The resistivity structure of high-temperature geothermal systems in Iceland. *Proceedings of the World Geothermal Congress 2000, Kyushu-Tohoku, Japan,* 923-928.

Badilla, D., 2011: *Appendices to the report " Resistivity imaging of the Santa Maria sector and the northern zone of Las pailas geothermal area, Costa Rica, using joint 1d inversion of TDEM and MT data"* UTP-GTP, Iceland, report 8, appendices, 45 pp.

Barrantes, M., 2006: Geo-environmental aspects for the development of Las Pailas geothermal field, Guanacaste, Costa Rica. Report 8 in: *Geothermal Training in Iceland 2006*. UNU-GTP, Iceland, 121-151.

Chavarría, L., Mora, O., Hakanson, E., Galvez, M., Rojas, M., Molina, F., and Murillo, A., 2010: Geologic model of the Pailas geothermal field, Guanacaste, Costa Rica. *Proceedings of the World Geothermal Congress 2010, Bali, Indonesia*, 4 pp.

Chavarría, L., Mora, O., Hakanson, E., Molina, F., Vega, E., Torres, Y., Vallejos, O., Yock, A., Lezama, G., and Castro S., 2006: *Development strategies for Las Pailas geothermal field (in Spanish).* Consultors Panel, Instituto Costarricense de Electricidad, Guanacaste, Costa Rica, 40 pp.

DeMets, C., Gordon, R.G., Argus, D.F., and Stein, S., 1990: Current plate motions. *Geophys. J. Int., 101*, 425-478.

GeothermEx Inc., 2001: *Pre-feasibility studies of the Las Pailas geothermal project, Costa Rica*. Instituto Costarricense de Electricidad, report, San José.

Hersir, G.P., and Árnason, K., 2009: Resistivity of rocks. *Paper presented at the Short Course on Surface Exploration for Geothermal Resources, organized by UNU-GTP and LaGeo, Santa Tecla, El Salvador*, 8 pp.

Molina, F., 2000: Las Pailas geothermal area, Rincón de la Vieja volcano, Costa Rica. Report 13 in: *Geothermal Training in Iceland 2000.* UNU-GTP, Iceland, 267-284.

Phoenix Geophysics, 2009: *Data processing. User's guide*. Phoenix Geophysics, Ltd., Toronto.

Rowland, B.F., 2002: *Time-domain electromagnetic exploration.* Northwest Geophysical Associates, Inc., 6 pp.

Simpson, F., and Bahr, K. 2005: *Practical magnetotellurics*. Cambridge University Press, Cambridge, UK, 270 pp.